IEEE Access
Multidisciplinary | Rapid Review | Open Access Journal

Received November 9, 2019, accepted November 21, 2019, date of publication November 25, 2019,
date of current version December 9, 2019.

Digital Object Identifier 10.1109/ACCESS.2019.2955552

A Multiagent-Based Hierarchical Energy Management Strategy for Maximization of Renewable Energy Consumption in Interconnected Multi-Microgrids

WEI JIANG[1], KAIXU YANG[1], JUNJIE YANG[2], RONGWEI MAO[3], NAIFAN XUE[1], AND ZHUHANG ZHUO[1]

[1]College of Electronics and Information Engineering, Shanghai University of Electric Power, Shanghai 200082, China
[2]School of Electronic Information Engineering, Shanghai Dianji University, Shanghai 201306, China
[3]Electrical Engineering and Computer Science, University of California Irvine, Irvine, CA 92697, USA

Corresponding author: Wei Jiang (shiepjw@shiep.edu.cn)

This work was supported in part by the National Natural Science Foundation of China under Grant 61202369 and Grant 61572311, in part by the Shanghai Technology Innovation Project under Grant 17020500900, and in part by the Shuguang Program sponsored by Shanghai Education Development Foundation and Shanghai Municipal Education Commission under Grant 17SG51.

ABSTRACT A new energy management framework for multi-microgrid (MMG) systems composed of high renewable energy sources (RES) is proposed in this paper. In traditional energy management system (EMS), battery energy storage system (BESS) is only considered in a single microgrid (MG) optimization model, which leads to underutilization of storage devices and waste of resources. Considering the advantages of local consumption of RES, this paper develops a hierarchical multi-agent energy management strategy. A two-step model aiming at maximizing the usage of RES is established to help determine the strategy. In the first step, the strategy is developed to maximize the local consumption of RES based on the demand response programs (DRP) and BESS within the independent MG. In the second step, the community BESS and BESSs are used to share the RES of multiple MGs for increasing the utilization ratio of RES. Simultaneously, the output of each controllable distributed generator (CDG) and the transaction with power grid are determined through a distributed adjustable power generation plan query library (DGPS). Moreover, the simulation with a three-MG system proves that the strategy can effectively increase the utilization ratio of RES and reduce the transaction with power grid compared to the traditional strategy.

INDEX TERMS Demand response programs, energy management system, mixed integer linear programming, multiagent system, multi-microgrids.

NOMENCLATURE

SETS AND INDICIS

- t index of time slot.
- i index of microgrid.
- $\widehat{(\bullet)}$ index of variables in real-time market.
- $\widetilde{(\bullet)}$ index of variables in MMG optimization.

PARAMETERS

- PR_t^{buy}/PR_t^{sell} Buying/selling price.
- $P_{MG_i,t}^{PV}/P_{MG_i,t}^{WT}$ Forecasted output of PV / WT.
- $P_{MG_i,t}^{RES}$ Forecasted renewable power.
- $P_{MG_i,t}^{L}$ Forecasted electricity load.
- $\overline{P}_{MG_i}^{PV}/\overline{P}_{MG_i}^{WT}$ Upper limits of PV/WT power output.
- $\overline{P}_{MG_i}^{CDG}/\overline{P}^{CCDG}$ Upper limits of CDG/CCDG power output.
- $\rho_{MG_i}^{CDG}$ Ramping up limits of CDG.
- $a_1/a_2/a_3$ Cost coefficients of CDG.
- $C_{MG_i}^{CDG\_star}/C_{MG_i}^{CCDG\_star}$ Star up cost of CDG/CCDG.
- $\overline{W}_{MG_i}^{CDG}$ Upper limits of greenhouse gas emissions.
- $f_{MG_i}^{CDG}$ emission coefficient of CDG.
- PR^{fu} Price of fuel.
- PR^{EN} the macroeconomic price of CO_2 reduction.

The associate editor coordinating the review of this manuscript and approving it for publication was Amjad Anvari-Moghaddam.

$E^{B}_{MG_i}$	Rated capacity of BESS.
$\overline{P}^{B+}_{MG_i}/\overline{P}^{B-}_{MG_i}$	Upper limits of BESS charging/discharging power.
$\eta^{B+}_{MG_i}/\eta^{B-}_{MG_i}$	BESS charging/discharging efficiencies.
$\overline{dr}_{MG_i}/\overline{inc}_{MG_i}$	maximum ratio of reduced/incresed load.
α_1/α_2	The weighting factor of objective function.
$\Delta t/\Delta\widehat{t}$	The time duration for converting power to energy.

VARIABLES

$P^{NL}_{MG_i,t}$	The net load.
P^{va}_{t}	Shortage power input value of DGPS.
$\mu^{CDG}_{MG_i,t}$	Commitment status indicator of a CDG.
$v^{CDG}_{MG_i,t}$	Status change indicator of a CDG.
$P^{CDG}_{MG_i,t}/P^{CCDG}_{t}$	CDG/CCDG power output.
$W^{CDG}_{MG_i,t}/W^{CCDG}_{MG_i,t}$	The amount of greenhouse gas emissions.
$\gamma^{B+}_{MG_i,t}/\gamma^{B-}_{MG_i,t}$	BESS charging/discharging indicator.
$P^{B+}_{MG_i,t}/P^{B-}_{MG_i,t}$	BESS charging/discharging power.
P^{CB+}_{t}/P^{CB-}_{t}	CBESS charging/discharging power.
$SOC^{B}_{MG_i,t}$	BESS state of charge.
$P^{dL}_{MG_i,t}$	Electricity load after applying DRP.
$P^{L+}_{MG_i,t}/P^{L-}_{MG_i,t}$	Increased/reduced load during DRP.
$dr_{MG_i,t}/inc_{MG_i,t}$	Ratio of reduced/incresed load.
$P^{sur}_{MG_i,t}/P^{va}_{MG_i,t}$	Surplus/shortage power in MG optimization.
$P^{buy}_{MG_i,t}/P^{sell}_{MG_i,t}$	power purchase from / sell to the power grid.
$C^{CDG}_{MG_i,t}/C^{CCDG}_{MG_i,t}$	Operation cost of CDG/CCDG.
$C^{CDG\_star}_{MG_i,t}$	Star up cost of CDG.
C^{EN}_{t}/C^{CG}_{t}	The total environmental / power generation cost of CDGs.
$C^{tr}_{MG_i,t}/C^{rer}_{MG_i,t}$	Transaction/renewable energy residual cost in MG optimization.

I. INTRODUCTION

Under the social background with the energy shortage and environmental pollution, RES such as wind energy, solar energy are the most important substituted energy sources which are being the main energy of modern power systems [1]. Renewable energy is dispersively connected into the distribution networks at present, and the adoption of local consumption has been the trend of its development. MG is a combination of distributed energy, energy storage system, loads and other equipments [2]. The different forms of power generation and electricity consumption unit are connected into the distribution networks as smart nodes with bidirectional scheduling capability, realizing the maximum benefit in grid-tied mode and improving reliability of system towards various accidents in island mode, while satisfying the user requirement [3], [4]. Hence, MG is the key part of the power grid transition from the existing grid to the future smart grid [5]. With the increasing penetration of distributed energy and the facts that uncertainties of both supply and demand in MG, MMG system is designed to handle those problem. The integration of interconnected MGs' resources and the interaction with the distribution network are common in the future smart distribution system [6], [7]. The cooperation of MMG system is favorable to the reasonable distribution of energy, the optimization of network operation costs and the improvement of power grid reliability [8].

Energy management system (EMS) is used for optimally scheduling power resources and energy storage systems in multi-microgrids to maintain supply-demand balance [9]. A lot of research has sought to introduce the algorithm and optimization models for the MMG EMS. In [10], [11], a control strategy for the coordinated operation of networked MGs in a distribution system is proposed. They formulate the problem as a stochastic bi-level optimization problem in which the upper level problem is solved by the distribution operator in order to guarantee the operational constraints while the lower level problem is to minimize the operation costs of MGs. However, the storage devices are not considered. In [12]–[14], the authors present a bilevel optimal operation model for distribution networks with grid-connected MGs. The upper-level model determines the optimal dispatch of the distribution network to achieve its power loss reduction and voltage profile improvement, while the lower-level model determines the optimal operation strategy of distributed generators in MGs considering the utilization of renewable power. However, in [12], although the operation of multiple grid-connected MGs are considered, only the interaction between the distribution network and MGs is studied without considering any power exchange among MGs. By contrast, in [13], [14], the cooperative interaction between MGs and energy storage systems is also taken into account. Specifically, the cooperation among MGs is modeled by an interactive energy game matrix based on priority-based game theory to take full advantage of energy storage systems. Moreover, the authors in [14] introduce the responsive reserve of distributed generators to the model to improve the system operation. Additionally, in [15], a distributed algorithm for the energy management of networked MGs based on the on-line alternating direction method of multipliers algorithm is proposed. Their objective is to coordinate the power scheduling of various components in the MGs while satisfying the underlying power network operation constraints. As reported by [16], in order to minimize the MGs operational costs, a decentralized markov decision based process has been presented. Multiagent system (MAS) has many features such as autonomous, communication, which realizes the bidirectional alternation of MGs' data and energy. From the aspects of modeling method, control, communication, energy coordination, etc., the application of MAS in distributed coordination control and optimization for micro-grid and multi-micro network is discussed [17]. A multiagent-based hierarchical

TABLE 1. Contribution comparison between our paper and related works.

Y/N	This study	[10] [11]	[15]	[12]	[13] [14]	[19] [29] [21]
BESS participates in MG optimization	Y	N	N	Y	Y	Y
BESS participates in MMG optimization	Y	N	N	N	N	N
CBESS participates in MMG optimization	Y	N	N	N	N	Y
Power exchange between the power grid and MGs	Y	Y	N	Y	Y	Y
Power exchange among MGs	Y	N	Y	Y	Y	Y
DC energy exchange network	Y	N	N	N	N	N
The CDGs have reconfigurability	Y	N	N	N	N	N
Optimization goals: operate costs	Y	Y	Y	Y	Y	Y
Optimization goals: the residual cost of renewable energy	Y	N	N	N	N	N
Consider the uncertainty in the day-ahead operation	N	N	N	N	N	Y
Consider the uncertainty in the real-time operation	Y	N	N	N	N	N

EMS which considers DRP and distributed storage system has been used to minimize the cost of electricity and reduce the system peak demand [18], [19]. MMG system requires the optimal operation of MGs with uncertainty management taken into account. Under the circumstance, a robust optimization based scheduling method for multi-microgrids considering uncertainties in RESs and forecasted electric loads is designed [20], [28].

Compared with related works, this paper has some improvements in different aspects. The contribution comparison between this paper and related works is shown in Table 1.

Review of the literature has identified that there are still some issues to be improved in the scheduling and dispatching of MGs. With the increasing penetration of renewable energy resources, the BESSs are becoming more and more important. In [12]–[14], BESS only participates in MG layer optimization, and ignores the remaining available capacity that can be utilized in MMG layer optimization. In [19], [21], the most remarkable one is that though the energy exchange of grid-MGs/MG-MG in those literature have considered. Specifically, they only allow exchange energy through the traditional AC distribution network. In contrast, the DC power lines enable the direct energy exchange among MGs. In [10], [11], [15], all CDGs are running in MG optimization under any circumstance, which leads to increase equipment operating costs. Most of the optimization goals are to minimize operating costs, which are not an excellent in some cases. In [20], [24], [28], although the uncertainty of RESs is considered in MMG system, the authors only consider it in day-ahead scheduling and ignore the RESs dynamic fluctuations in real-time operation.

In order to address the above issues, this paper presents a multiagent hierarchical energy management strategy for interconnected multi-microgrids. From the Fig. 1, we can see that each MG is connected to the traditional AC distribution network and at the same time, they are interconnected by a dedicated DC power lines. The AC power lines can provide sufficient energy. The DC power lines enables the direct energy exchange among MGs and the connection to the distribution network by DC/AC converter can ensure that the surplus renewable energy is uniformly uploaded to the power grid. Compared with previous multi-microgrids energy management strategy [10]–[15], [19]–[21], [24], the features of energy management strategy proposed in this paper are summarized as follows:

- *In addition to participating in MG layer optimization, BESS of each MG also participates in MMG layer optimization. The purpose is to increase consumption of renewable energy by taking full advantage of BESS remaining available capacity.*
- *Considering maximizing local consumption of renewable energy in day-ahead scheduling control based on a hierarchical optimization method, renewable energy residual costs are added to the optimization goals.*
- *Rule-based energy scheduler is proposed in real-time scheduling, Based on the MMG system architecture, the energy management for the coordination between the DC power lines and the AC power lines can effectively cope with uncertainty.*
- *In the face of the shortcomings of always running all CDGs to participate in MG optimization under any circumstances, the concept of "distributed adjustable power generation plan query library" is proposed. It is a database that can find the best match and output of CDGs based on the power shortage.*

This paper is organized as follows. Section II presents the energy management strategies. Section III introduces the model for day-ahead scheduling. Section IV describes the numerical simulations and discussion. Section V concludes the paper.

II. ENERGY MANAGEMENT STRATEGIES

Configuration and components of MMG system under consideration is outlined in this section.

A. SYSTEM DESCRIPTION

The MMG system, composed of three MGs (MG1, MG2, MG3) and community MG (CMG), is used in this study in order to study the problem of the renewable energy consumption. The structure of the system is shown in Fig. 1. Each MG contains a BESS, CDG, photovoltaic (PV), wind turbine (WT), and electrical load. CMG is the shared dis-

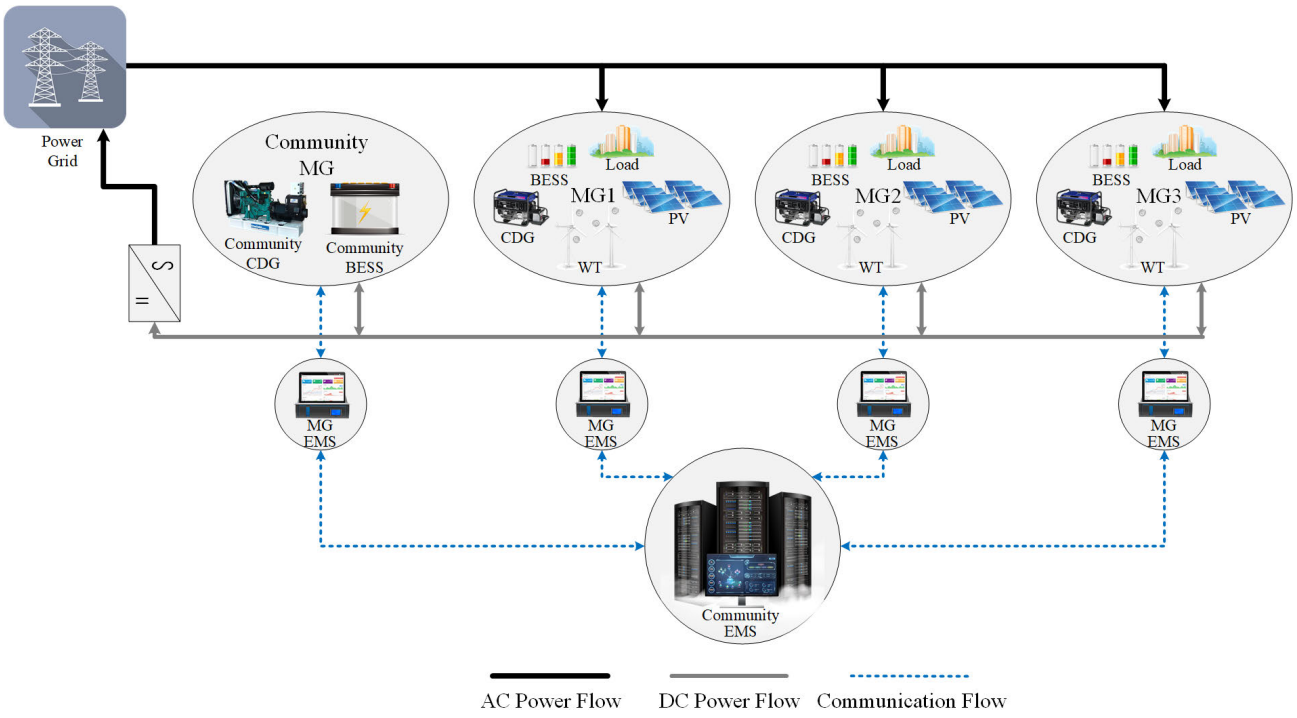

FIGURE 1. The structure of proposed MMG system.

tributed energy resources, which is comprised of community CDG (CCDG) and community BESS (CBESS). In MMG system, each MG is connected to the power grid via the AC bus and can receive power in real time; all MGs and CMG are connected via the DC bus and execute renewable energy transactions. In addition, MMG's surplus renewable energy is delivered to the power grid through the DC/AC converter. To ensure higher utilization ratio of renewable energy, it is assumed that the storage devices do not store energy by charging from the power grid.

B. SYSTEM MODEL

1) PV AND WT

PV and WT are considered as uncontrollable power generation units due to their stochastic output power. The historical forecast data in day-ahead market are used as correlated scenarios in this paper. $P^{PV}_{MG_i,t}$ and $P^{WT}_{MG_i,t}$ are the forecasted output of PV / WT (in kW), and they should satisfy the following power limits.

$$0 \le P^{PV}_{MG_i,t} \le \overline{P}^{PV}_{MG_i} \tag{1}$$

$$0 \le P^{WT}_{MG_i,t} \le \overline{P}^{WT}_{MG_i} \tag{2}$$

where $\overline{P}^{PV}_{MG_i}$ and $\overline{P}^{WT}_{MG_i}$ are the upper limits of PV/WT power output (in kW).

$P^{RES}_{MG_i,t}$ is the forecasted renewable power of MGi in t (in kW).

$$P^{RES}_{MG_i,t} = P^{PV}_{MG_i,t} + P^{WT}_{MG_i,t} \tag{3}$$

2) CDG

It is assumed that a diesel generator is controllable power generation unit, which can produce energy based on the reference value. In this paper, a diesel generator is used to represent CDG. $P^{CDG}_{MG_i,t}$ is CDG power output (in kW), and it should satisfy the following constraints.

$$0 \le P^{CDG}_{MG_i,t} \le \mu^{CDG}_{MG_i,t} \cdot \overline{P}^{CDG}_{MG_i} \tag{4}$$

$$\mu^{CDG}_{MG_i,t} \in \{0, 1\} \tag{5}$$

$$|P^{CDG}_{MG_i,t} - P^{CDG}_{MG_i,t-1}| \le \rho^{CDG}_{MG_i} \cdot \overline{P}^{CDG}_{MG_i} \tag{6}$$

The generation limit and ramp up rate constraints for a diesel generator are illustrated in Equations (4)-(6). $\overline{P}^{CDG}_{MG_i}$ represent upper limits of CDG power output (in kW). $\mu^{CDG}_{MG_i,t}$ is a binary variable indicating on/off status of generator. $\rho^{CDG}_{MG_i}$ represents ramp up limits of CDG.

$C^{CDG}_{MG_i,t}$, the cost of a diesel generator (in \$), can be formulated as in equation (7). At the same time, $C^{CDG\_star}_{MG_i,t}$ as a star up cost (in \$) is considered in equation (8).

$$C^{CDG}_{MG_i,t} = a_1 \cdot (P^{CDG}_{MG_i,t})^2 + a_2 \cdot P^{CDG}_{MG_i,t} + a_3 \tag{7}$$

$$C^{CDG\_star}_{MG_i,t} = v^{CDG}_{MG_i,t} \cdot C^{CDG\_star}_{MG_i} \tag{8}$$

$$v^{CDG}_{MG_i,t} = \max\{(\mu^{CDG}_{MG_i,t} - \mu^{CDG}_{MG_i,t-1}), 0\} \tag{9}$$

where a_1, a_2 and a_3 are generator cost function coefficients. $v^{CDG}_{MG_i,t}$ represents the change in the status of generator.

A diesel generator uses oil, which is fossil fuels. At the same time, it can release harmful gases such as sulfur, nitrogen and carbon oxides, and cause environmental pollution.

Thus, the cost of pollution is considered in this paper. $W^{CDG}_{MG_i,t}$, the amount of greenhouse gas emissions (in tCO_2), relies on the amount of used fuel in the diesel generator. so it is calculated using equation (10).

$$W^{CDG}_{MG_i,t} = f^{CDG}_{MG_i} \cdot \frac{C^{CDG}_{MG_i,t}}{PR^{fu}} \tag{10}$$

In above equations, $f^{CDG}_{MG_i}$ is the emission coefficient of the generator (in tCO_2/m^3), which depends on the fuel type and generator characteristics. PR^{fu} is the fuel price of generator (in $\$/m^3$).

Equation (11) is restriction about the amount of the carbon dioxide. $\overline{W}^{CDG}_{MG_i}$ is the maximum value of MGi allowed (in tCO_2).

$$\sum W^{CDG}_{MG_i,t} \le \overline{W}^{CDG}_{MG_i} \tag{11}$$

3) BESS

In practice, various storage systems have their own characteristics. $E^{B}_{MG_i}$, the maximum energy storage capacity (in kWh), is used for a battery model:

$$E^{B}_{MG_i} = A^{B}_{MG_i} \cdot V^{B}_{MG_i} \tag{12}$$

where $A^{B}_{MG_i}$ is the current-hour(Ah) rating of the battery, and $V^{B}_{MG_i}$ (in V) is the maximum voltage of the battery when it is fully charged (100% state of charge).

The operation of BESS should meet the following constraints.

$P^{B+}_{MG_i,t}$ and $P^{B-}_{MG_i,t}$ represent BESS charing and discharging power (in kW). Equation (13) and (14) limit BESS charing and discharging power capacity.

$$0 \le P^{B+}_{MG_i,t} \le \gamma^{B+}_{MG_i,t} \cdot \overline{P}^{B+}_{MG_i} \tag{13}$$

$$0 \le P^{B-}_{MG_i,t} \le \gamma^{B-}_{MG_i,t} \cdot \overline{P}^{B-}_{MG_i} \tag{14}$$

$$\gamma^{B+}_{MG_i,t} + \gamma^{B-}_{MG_i,t} \le 1 \tag{15}$$

$$\gamma^{B+}_{MG_i,t}, \gamma^{B-}_{MG_i,t} \in \{0, 1\} \tag{16}$$

where $\overline{P}^{B+}_{MG_i}$ and $\overline{P}^{B-}_{MG_i}$ are the upper limits of BESS charging and discharging power (in kW), respectively. Equation (15) means that BESS cannot operate in charging mode and discharging mode simultaneously. $\gamma^{B+}_{MG_i,t}$ and $\gamma^{B-}_{MG_i,t}$ are the state of BESS charing and discharging in t (=1,charing/discharging; =0, otherwise).

Equation (17) shows the change of electricity stored in BESS at $t > 1$, which includes net energy injection and energy losses during charging/discharging process.

$$SOC^{B}_{MG_i,t} = SOC^{B}_{MG_i,t-1} + \frac{1}{E^{B}_{MG_i}}\left(P^{B+}_{MG_i,t} \cdot \Delta t \cdot \eta^{B+}_{MG_i} - \frac{P^{B-}_{MG_i,t} \cdot \Delta t}{\eta^{B-}_{MG_i}}\right) \tag{17}$$

where $SOC^{B}_{MG_i,t}$ is BESS state of charge (SOC) at time t. $\eta^{B+}_{MG_i}$ and $\eta^{B-}_{MG_i}$ are the charging and discharging efficiencies. Δt is the time duration for converting power to energy.

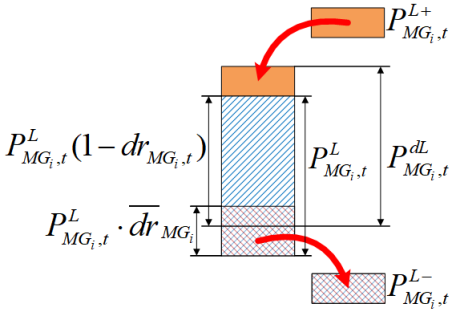

FIGURE 2. Modeling participated load in DRP.

The limit and initial of SOC in a BESS is constrained by equations (18) and (19).

$$0 \le SOC^{B}_{MG_i,t} \le 1 \tag{18}$$

$$SOC^{B}_{MG_i,t=1} = SOC^{B}_{MG_i,initial} \tag{19}$$

4) LOAD

Two types of loads are considered in MG: shiftable load and fixed load. Shiftable loads can be shifted in time, but a definite amount of energy must be consumed in the planning horizon. On other hand, fixed loads are critical loads, which are not allowed to be shifted or shedded. $P^{L-}_{MG_i,t}$, the amount of shiftable loads from interval t to other time (in kW), is shown by the Equation (20).

$$P^{L-}_{MG_i,t} = dr_{MG_i,t} \cdot P^{L}_{MG_i,t} \tag{20}$$

$$0 \le dr_{MG_i,t} \le \overline{dr}_{MG_i} \tag{21}$$

In above equations, $P^{L}_{MG_i,t}$ indicates the primary electric loads in interval t (in kW). $dr_{MG_i,t}$ and $\overline{dr}_{MG_i}$ represents the percentage factor of load shifting from hour t and its maximum value.

C. CONCEPTS: TERMINOLOGIES AND DEFINITIONS

1) DRP

The aim of DRP is to shift the shiftable load from high electricity price time intervals to the low electricity price time intervals. So each MG will adjust their shiftable loads regarding to day-ahead forecasting electricity price in order to minimize purchase cost as well as maximizing sale profit. It is noted that each MG can shift only the limited portion of the load which can be different during scheduling horizon. Modeling participated load in DRP is illustrated by Fig. 2. $P^{L+}_{MG_i,t}$ is the shiftable loads from other time intervals to interval t (in kW). $P^{dL}_{MG_i,t}$, the load after applying DRP (in kW), can be formulated as:

$$P^{dL}_{MG_i,t} = (1 - dr_{MG_i,t}) \cdot P^{L}_{MG_i,t} + P^{L+}_{MG_i,t} \tag{22}$$

To prevent the excessive shift of load in the intervals, the increased load $P^{L+}_{MG_i,t}$ in each interval (in kW) is limited by the following constraint:

$$P^{L+}_{MG_i,t} = inc_{MG_i,t} \cdot P^{L}_{MG_i,t} \tag{23}$$

$$0 \le inc_{MG_i,t} \le \overline{inc}_{MG_i} \tag{24}$$

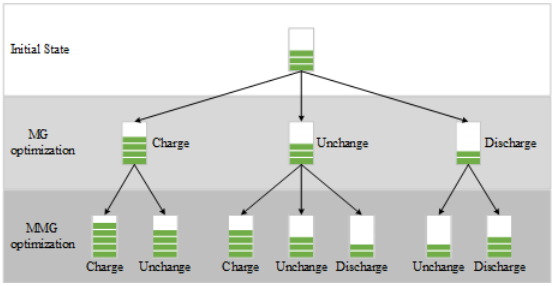

FIGURE 3. All changes of BESS state.

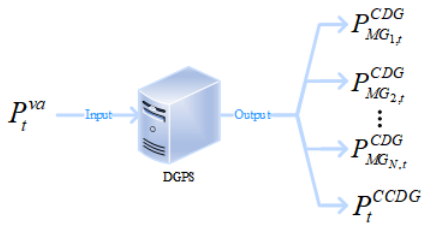

FIGURE 4. Distributed power generation plan come from query library.

where $inc_{MG_i,t}$ and $\overline{inc}_{MG_i}$ represents the incremental factor and its maximum value.

For the load, the total daily consumed energy of MG will be the same before and after applying DRP, which can be defined by the Equation (25).

$$\sum_{t=1}^{24} P_{MG_i,t}^{L-} = \sum_{t=1}^{24} P_{MG_i,t}^{L+} \tag{25}$$

2) STATE CHANGE OF BESS

BESS has three state changes: charge, unchange, and discharge. Since BESS cannot be charged and discharged at the same time, all possible state changes of BESS in the day-ahead two-level scheduling is shown in Fig. 3. From the Fig. 3, we can see that BESS state of MMG optimization is affected by BESS state of MG optimization. For example, if BESS state of MG optimization is charged, in MMG optimization, its state can only be one of the two state (charge or unchange). so here is one of the constraints of BESS in MMG optimization.

3) DGPS

DGPS is a database which have 1-to-1 mappings between the input value and the output value. Fig. 4 shows that the corresponding power output of CDGs can be queried by entering P_t^{va} into the database.

C_t^{CG} and C_t^{EN} indicate the total power generation cost and environmental cost of CDGs.

$$C_t^{CG} = \sum_{i}^{N} (C_{MG_i,t}^{CDG} + C_{MG_i,t}^{CDG\_star}) + C_t^{CCDG} + C_t^{CCDG\_star} \tag{26}$$

$$C_t^{EN} = (\sum_{i}^{N} W_{MG_i,t}^{CDG} + W_{MG_i,t}^{CCDG}) \cdot PR^{EN} \tag{27}$$

where PR^{EN} is the macroeconomic cost of CO_2 reduction (in \$/t).

Objective function: Considering the total power generation cost and environmental cost, the best cooperative power generation schedule for all CDGs under all circumstances is developed, which utilized for minimizing the operational cost of MMG system and avoid unnecessary trading with the power grid. Equation (28) is the objective function.

$$minf_1 = \alpha_1 C_t^{CG} + \alpha_2 C_t^{EN} \tag{28}$$

In order to solve multi-objective optimization, a weighting method is used to integrate the two objectives into one objective.where α_1, α_2 are the weighting factor according to the importance degree of the optimization goal, and their sum is 1. In this study, $\alpha_1 = 0.6, \alpha_2 = 0.4$.

Constraints: Some equality and inequality constraints should be met.

The generation of CDGs is limited in Equation (4)-(11).

P_t^{va} is the shortage power of MMG system (in kW) which is a independent variable. Equation (29) indicates that its range of values contains all possible conditions in the database. Equation (30) shows the equivalent relationship between input and output.

$$0 \le P_t^{va} \le \sum_{i=1}^{N} P_{MG_{i,t}}^{CDG_{max}} + P_t^{CCDG_{max}} \tag{29}$$

$$P_t^{va} = \sum_{i=1}^{N} P_{MG_{i,t}}^{CDG} + P_t^{CCDG} \tag{30}$$

where $P_{MG_{i,t}}^{CDG}$ and $P_{MG_{i,t}}^{CDG_{max}}$ represent the output power (in kW) and its upper limits of CDG (in kW). P_t^{CCDG} and $P_t^{CCDG_{max}}$ represent the output power (in kW) and its upper limits of CCDG (in kW).

4) RULE-BASED ENERGY SCHEDULER

In real-time dispatch, a rule based energy scheduler was carried out to solve uncertainties (i.e. RES and Load) in MG. It is determined by the actual measured and predicted value of the net load (load minus the amount of renewable energy generated) and is addressed by coordinating energy management between the DC/AC power line and the grid. Note that the real-time dispatch interval could be any short uniform time interval (e.g. 1-second interval). In this paper, the proposed dispatching interval is assumed to be 1 s ($\Delta\hat{t} = 1s$). As the time scale is 1 s, the time window of the dispatch covers 86400 intervals (i.e. 24h). $\hat{t} \in \{1, 2, \ldots, RT\}$ $RT = 86400$. In day-ahead dispatch, the proposed dispatching interval is assumed to be 1 hour ($\Delta t = 1h$). $t \in \{1, 2, \ldots, T\}$ $T = 24$.

The net load (in kW) at the time t is presented by the equation (31).

$$P_{MG_i,t}^{NL} = P_{MG_i,t}^{dL} - P_{MG_i,t}^{RES} \tag{31}$$

$$\hat{P}_{MG_i,\hat{t}}^{NL} = \hat{P}_{MG_i,\hat{t}}^{L} - \hat{P}_{MG_i,\hat{t}}^{RES} \tag{32}$$

where $P_{MG_i,t}^{NL}$ is the day-ahead prediction of the net load. Note that ($\hat{\bullet}$) is used to denote the variables in real time market.

Algorithm 1 Real-Time Processing of Prediction Error

Input: $P^{NL}_{MG_i,t}$, $\widehat{P}^{NL}_{MG_i,\widehat{t}}$, $P^{buy}_{MG_i,t}$ and $P^{sell}_{MG_i,t}$
Output: $\widehat{P}^{buy}_{MG_i,\widehat{t}}$ and $\widehat{P}^{sell}_{MG_i,\widehat{t}}$
Running Rule-based energy scheduler;
while $\widehat{t} \leq RT$ **do**
  $t = T \cap [\frac{\widehat{t}}{3600}, \frac{\widehat{t}}{3600} + 1)$;
  $E^{NL}_{MG_i,\widehat{t}} = \frac{P^{NL}_{MG_i,t} \cdot \Delta t}{3600}$;
  $\widehat{E}^{NL}_{MG_i,\widehat{t}} = \widehat{P}^{NL}_{MG_i,\widehat{t}} \cdot \Delta\widehat{t}$;
  $E^{buy}_{MG_i,\widehat{t}} = \frac{P^{buy}_{MG_i,t} \cdot \Delta t}{3600}$;
  $E^{sell}_{MG_i,\widehat{t}} = \frac{P^{sell}_{MG_i,t} \cdot \Delta t}{3600}$;
  if $E^{NL}_{MG_i,\widehat{t}} \leq \widehat{E}^{NL}_{MG_i,\widehat{t}}$ **then**
    $a = \widehat{E}^{NL}_{MG_i,\widehat{t}} - E^{NL}_{MG_i,\widehat{t}}$;
    if $0 \leq a < E^{sell}_{MG_i,\widehat{t}}$ **then**
      $\widehat{P}^{buy}_{MG_i,\widehat{t}} = \frac{E^{buy}_{MG_i,\widehat{t}}}{\Delta\widehat{t}}$;
      $\widehat{P}^{sell}_{MG_i,\widehat{t}} = \frac{E^{sell}_{MG_i,\widehat{t}} - a}{\Delta\widehat{t}}$;
    else if $E^{sell}_{MG_i,\widehat{t}} \leq a$ **then**
      $\widehat{P}^{buy}_{MG_i,\widehat{t}} = \frac{E^{buy}_{MG_i,\widehat{t}} + (a - E^{sell}_{MG_i,\widehat{t}})}{\widehat{t}}$;
      $\widehat{P}^{sell}_{MG_i,\widehat{t}} = 0$;
    end
  else
    $a = E^{NL}_{MG_i,\widehat{t}} - \widehat{E}^{NL}_{MG_i,\widehat{t}}$;
    if $0 \leq a < E^{buy}_{MG_i,\widehat{t}}$ **then**
      $\widehat{P}^{buy}_{MG_i,\widehat{t}} = \frac{E^{buy}_{MG_i,\widehat{t}} - a}{\Delta\widehat{t}}$;;
      $\widehat{P}^{sell}_{MG_i,\widehat{t}} = \frac{E^{sell}_{MG_i,\widehat{t}}}{\Delta\widehat{t}}$;
    else if $E^{buy}_{MG_i,\widehat{t}} \leq a$ **then**
      $\widehat{P}^{buy}_{MG_i,\widehat{t}} = 0$;
      $\widehat{P}^{sell}_{MG_i,\widehat{t}} = \frac{E^{sell}_{MG_i,\widehat{t}} + (a - E^{buy}_{MG_i,\widehat{t}})}{\widehat{t}}$;
    end
  end
  $\widehat{t}++$;
end

MGA calculates $\widehat{P}^{buy}_{MG_i,\widehat{t}}$ and $\widehat{P}^{sell}_{MG_i,\widehat{t}}$ (power purchased from / sold to power grid in real-time operation scheduling) based on $P^{buy}_{MG_i,t}$ and $P^{sell}_{MG_i,t}$(power purchase from / sell to the power grid in day-ahead operation) according to Algorithm 1.

D. MULTI AGENT SYSTEM STRUCTURE

The structure of the proposed MMG hierarchical MAS is shown in Fig. 5. The communication between the agents and the time sequence they take place are contained in this figure. The agents are briefly described in accordance to the nature of the task they are responsible for.

1) LOCAL AGENTS

Local agents that are responsible to represent a single component of MMG system, such as PV agent, WT agent, Load agent, BESS agent, CDG agent, CBESS agent, CCDG agent. These are responsible for communicating with their MG agent to upload relevant data and receiving operational commands.

2) MG AGENT

MG agent (MGA), which is MG EMS, performs MG layer optimization based on the data from local agents and uploads the result of MG optimization (surplus/shortage power as well as the energy storage status information) to the MMG agent. In addition, it also inform the local agents about the state of operation change commands from MMG agent.

3) MARKET AGENT

Market agent (MA) is responsible for providing the day-ahead buying and selling prices signals for MMG agent.

4) MMG AGENT

MMG agent (MMGA), which is community EMS, is responsible for the global optimization of MMG system. It receives all the information from MA and MGA and inform the state of operation change commands to MGA.

The communication between agents is shown in Fig. 5. Firstly, a message about getting the forecast market price signals is sent by MMGA to MA. MA sends the forecast buying and selling prices to MMGA. Secondly, The information (info) request about MG optimization results and the forecast market price signals from MMGA are destined to MGA. Thirdly, each MGA will inform its local agents about the information request messages, such as the forecast power of PV, WT, and Load and the initial value of BESS/CBESS. Based on the information replied from their local agent, each MGA will perform MG layer optimization. The result of MG optimization is calculated in Algorithm 2. Fourthly, All the MGA will reply the MMGA about the result of MG optimization/the initial value of CBESS. Based on the information replied from all the MGA, MMGA will perform MMG layer optimization. The result of MMG optimization is calculated in Algorithm 3. At last, MMGA will inform MGA about the state of operation change commands and Respective MGA will inform their local agents about the state of operation change commands.

E. PROPOSED STRATEGIES

With high renewable penetration, MMG system has the ability to make full use of renewable energy. A multiagent-based hierarchical energy management strategy, with demand side management and power scheduling in interconnected MMGs, is shown in Fig. 6.

The proposed operation framework have two operation module: Day-ahead operation module and real-time operation module. MG optimization and MMG optimization are

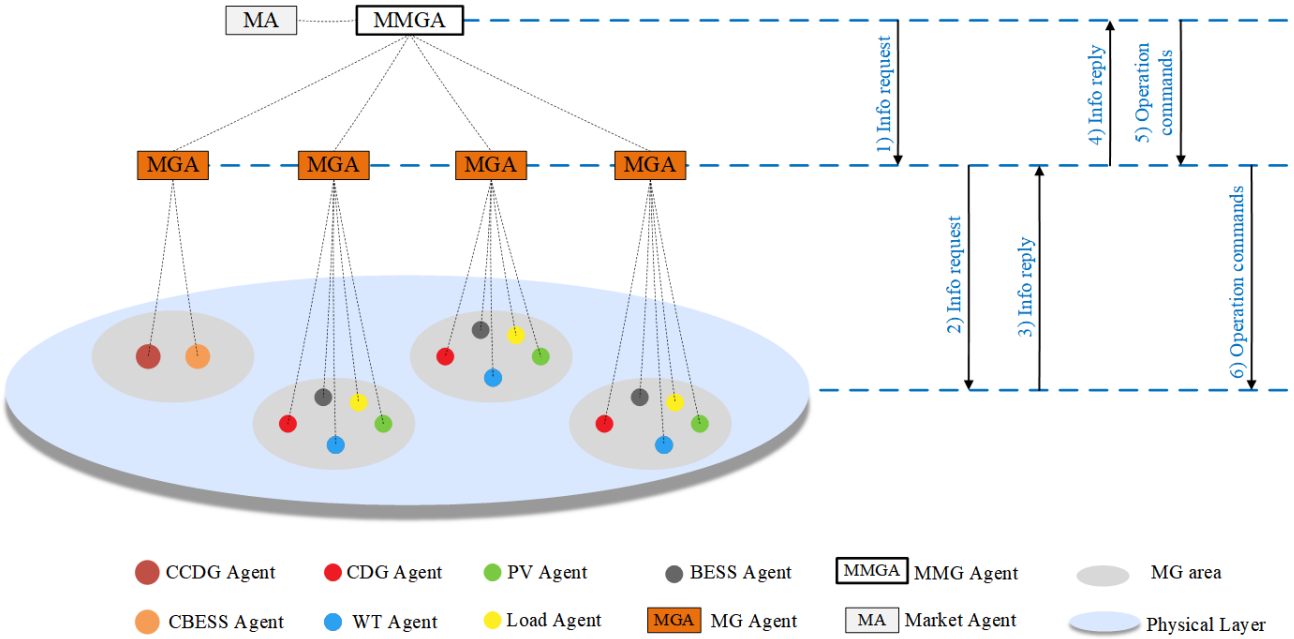

FIGURE 5. The structure of proposed hierarchical MAS.

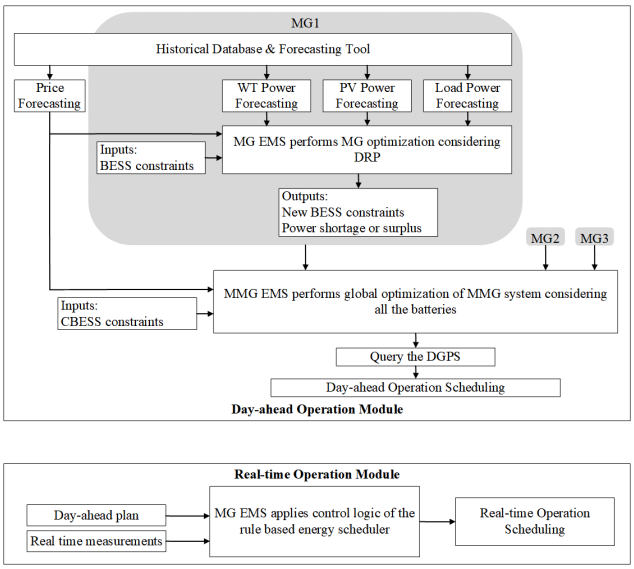

FIGURE 6. Proposed operation framework.

included in the day-ahead operation module. The objective of the proposed day-ahead energy scheduling is maximizing the renewable energy consumption to identify the optimal amount of electricity to be purchased from/sold to the power grid and the commitment of CDGs over the next 24 hours. In MG optimization, renewable power generation, electricity load and electricity price are predicted based on historical database and forecasting tools. Considering DRP, the shiftable load and BESS are utilized by MG EMS to perform demand side optimization management. The objective of optimization is to maximize local renewable energy consumption, as well as minimize the cost of power exchange based on the day-ahead electricity price. In MMG optimization, Firstly, community BESS and all MG's BESS are utilized by MMG EMS to perform MMG optimization based on the load deficiencies and renewable energy surplus information uploaded by each MG EMS. The objective of optimization is to further consume renewable energy. Then, DGPS performs judgment based on the optimized power information. If the power is short, the optimal generation plan for CDGs and purchase amount from power grid through the AC bus can be obtained. Otherwise, excess renewable energy will be sold to the power grid through shared DC bus. A rule based energy scheduler is proposed in the real-time operation module. It is determined by the actual measured and predicted value of the net load (load minus the amount of renewable energy generated) and is addressed by coordinating energy management between the DC/AC power line and the grid.

III. HOURLY DAY-AHEAD OPTIMAL SCHEDULING MODEL

In this section, problem formulation is based on MILP. MILP problems can be easily implemented through commercial software like CPLEX, which guarantee global optimality.

The first step is MG optimization considering DRP carried out by MG EMS. The second step is MMG optimization, which contains two parts. That is, the global optimization of distributed energy storage and distributed controllable power generation is completed by community EMS. Mathematical models are established in the following sections in detail.

A. STEP 1: MG OPTIMIZATION

Considering maximizing consumption of renewable energy in day-ahead scheduling, $C^{rer}_{MG_{i,t}}$, renewable energy residual

cost is adopted. The calculation of $C^{rer}_{MG_{i,t}}$ is defined as:

$$C^{rer}_{MG_{i,t}} = P^{sur}_{MG_{i,t}} \cdot \Delta t \cdot max\{PR^{buy}_1, PR^{buy}_2, \ldots, PR^{buy}_{24}\} \quad (33)$$

where $P^{sur}_{MG_{i,t}}$ and $P^{va}_{MG_{i,t}}$ are the surplus power (in kW) and shortage power (in kW) in MG optimization. PR^{buy}_t and PR^{sell}_t are the price of power buying/selling (in \$/kWh).

$C^{tr}_{MG_{i,t}}$ indicates the transaction cost.

$$C^{tr}_{MG_{i,t}} = \begin{cases} P^{sur}_{MG_{i,t}} \cdot \Delta t \cdot PR^{sell}_t \\ when \sum_{t=1}^{T} (P^{RES}_{MG_{i,t}} - P^{L}_{MG_{i,t}}) \cdot \Delta t > 0 \\ P^{va}_{MG_{i,t}} \cdot \Delta t \cdot PR^{buy}_t \\ when \sum_{t=1}^{T} (P^{RES}_{MG_{i,t}} - P^{L}_{MG_{i,t}}) \cdot \Delta t < 0 \end{cases} \quad (34)$$

$\sum_{t=1}^{T} (P^{RES}_{MG_{i,t}} - P^{L}_{MG_{i,t}}) \cdot \Delta t$ is the difference of RE generation and load for the future $24h$. $C^{tr}_{MG_{i,t}}$ (in \$) conforms the constraints that when the load is higher than the RE generation, $C^{tr}_{MG_{i,t}}$ is equal to the cost of power bought from the power grid; when the load is lower than the RE generation, $C^{tr}_{MG_{i,t}}$ is equal to the profit of power sold to the power grid or other MGs.

Objective function: The objective of MG optimization is to maximize renewable energy consumption of individual MG, as shown below:

$$minf_2 = \sum_{t=1}^{T} \{\alpha_1 \cdot C^{rer}_{MG_{i,t}} + \alpha_2 \cdot C^{tr}_{MG_{i,t}}\} \quad (35)$$

Constraints: Some equality and inequality constraints should be met.

The generation of RE (PV and WT) is limited in Equation (1)-(3).

The operational constraints of a BESS are shown in Equation (12)-(19).

The constraints of load and DRP are specified in Equation (20)-(25).

For each MG, the balance between RE generation, shortage power, discharge power of BESS and surplus power, charge power of BESS, load after DRP is described by Equation (36).

$$(P^{RES}_{MG_{i,t}} + P^{va}_{MG_{i,t}} + P^{B-}_{MG_{i,t}}) \cdot \Delta t = (P^{sur}_{MG_{i,t}} + P^{B+}_{MG_{i,t}} + P^{dL}_{MG_{i,t}}) \cdot \Delta t \quad t \in T \quad (36)$$

After completing MG optimization by each MGA at step 1, each MGA calculates $P^{sur}_{MG_{i,t}}$, $P^{va}_{MG_{i,t}}$, $P^{B+}_{MG_{i,t}}$, $P^{B-}_{MG_{i,t}}$ and part of $\widetilde{P}^{B+}_{MG_{i,t}}/\widetilde{P}^{B-}_{MG_{i,t}}$ (some BESS determinable charge and discharge power in distributed energy storage optimization) according to Algorithm 2. The calculated values are communicated to the MMGA.

Algorithm 2 Computation of MG Optimization Result

Input: $P^{RES}_{MG_i}, P^{L}_{MG_i}, PR^{buy}_t, PR^{sell}_t$
Output: $P^{sur}_{MG_{i,t}}, P^{va}_{MG_{i,t}}, P^{B+}_{MG_{i,t}}, P^{B-}_{MG_{i,t}}$, part of $\widetilde{P}^{B+}_{MG_{i,t}}/\widetilde{P}^{B-}_{MG_{i,t}}$

```
Running MG optimization;
return P^{B+}_{MG_{i,t}}, P^{B-}_{MG_{i,t}}, P^{dL}_{MG_{i,t}};
while t ≤ T do
    if P^{RES}_{MG_{i,t}} ≤ P^{dL}_{MG_{i,t}} then
        P^{va}_{MG_{i,t}} = P^{dL}_{MG_{i,t}} − P^{RES}_{MG_{i,t}} − P^{B−}_{MG_{i,t}};
        P^{sur}_{MG_{i,t}} = 0;
        if P^{B+}_{MG_{i,t}} > 0 then
            P̃^{B−}_{MG_{i,t}} = 0;
        else if P^{B−}_{MG_{i,t}} > 0 then
            P̃^{B+}_{MG_{i,t}} = 0;
        end
    else
        P^{va}_{MG_{i,t}} = 0;
        P^{sur}_{MG_{i,t}} = P^{RES}_{MG_{i,t}} − P^{dL}_{MG_{i,t}} − P^{B+}_{MG_{i,t}};
        if P^{B+}_{MG_{i,t}} > 0 then
            P̃^{B−}_{MG_{i,t}} = 0;
        else if P^{B−}_{MG_{i,t}} > 0 then
            P̃^{B+}_{MG_{i,t}} = 0;
        end
    end
    t++;
end
```

B. STEP 2: MMG OPTIMIZATION

There are two-stage optimization of the community EMS. In the first stage, according to the surplus power, shortage power and the charge/discharge margin of BESS in each MG, the optimization of all the batteries in MMG system will be performed to further consumption of renewable energy. In the second stage, the generation schedule of all the CDG in MMG system is made based on the update of shortage power obtained from the first stage. Details of the two-stage optimization control are presented as follows:

1) DISTRIBUTED ENERGY STORAGE OPTIMIZATION

Similarly, the objective of this optimization is to further maximize renewable energy consumption of the MMG system. In the meantime, the BESS of each MG and community BESS participate in global optimization.

Objective function:

$$minf_3 = \sum_{i=1}^{N} \sum_{t=1}^{T} \{\alpha_1 \cdot \widetilde{C}^{rer}_{MG_{i,t}} + \alpha_2 \cdot \widetilde{C}^{tr}_{MG_{i,t}}\} \quad (37)$$

$$\widetilde{C}^{rer}_{MG_{i,t}} = \widetilde{P}^{sur}_{MG_{i,t}} \cdot \Delta t \cdot max\{PR^{buy}_1, PR^{buy}_2, \ldots, PR^{buy}_{24}\} \quad (38)$$

where $\widetilde{P}^{sur}_{MG_{i,t}}$ and $\widetilde{P}^{va}_{MG_{i,t}}$ are the surplus power (in kW) and shortage power (in kW) in distributed energy storage

optimization.

$$\widetilde{C}^{tr}_{MG_{i,t}} = \begin{cases} -\widetilde{P}^{sur}_{MG_{i,t}} \cdot \Delta t \cdot PR^{sell}_t \\ when \sum_{i=1}^{N}\sum_{t=1}^{T}(P^{sur}_{MG_{i,t}} - P^{va}_{MG_{i,t}}) \cdot \Delta t > 0 \\ \widetilde{P}^{va}_{MG_{i,t}} \cdot \Delta t \cdot PR^{buy}_t \\ when \sum_{i=1}^{N}\sum_{t=1}^{T}(P^{sur}_{MG_{i,t}} - P^{va}_{MG_{i,t}}) \cdot \Delta t < 0 \end{cases} \quad (39)$$

$\sum_{i=1}^{N}\sum_{t=1}^{T}(P^{sur}_{MG_{i,t}} - P^{va}_{MG_{i,t}}) \cdot \Delta t$ is the difference between the total surplus power and the total shortage power of MMG system after each MG optimization. $\widetilde{C}^{tr}_{MG_{i,t}}$ (in \$) conforms the constraints that when the total surplus power is higher than the total shortage power, $\widetilde{C}^{tr}_{MG_{i,t}}$ is equal to the cost of power bought from the power grid; when the total surplus power is lower than the total shortage power, $\widetilde{C}^{tr}_{MG_{i,t}}$ is equal to the profit of power sold to the power grid.

Constraints: Some equality and inequality constraints should be met.

The operational constraints of CBESS are shown in Equation (12)-(19).

Based on the state of the BESS after MG optimization, the new constraints of BESS are presented as follows.

$$0 \le \widetilde{P}^{B+}_{MG_{i,t}} \le \widetilde{\gamma}^{B+}_{MG_{i,t}} \cdot \overline{P}^{B+}_{MG_i} \quad (40)$$

$$0 \le \widetilde{P}^{B-}_{MG_{i,t}} \le \widetilde{\gamma}^{B-}_{MG_{i,t}} \cdot \overline{P}^{B-}_{MG_i} \quad (41)$$

where $\widetilde{P}^{B+}_{MG_{i,t}}$ and $\widetilde{P}^{B-}_{MG_{i,t}}$ represent BESS charing and discharging power (in kW) in distributed energy storage optimization. Equation (40) and (41) limit BESS charing and discharging power capacity. $\widetilde{\gamma}^{B+}_{MG_{i,t}}$ and $\widetilde{\gamma}^{B-}_{MG_{i,t}}$ are the state of BESS charing and discharging in distributed energy storage optimization (=1,charing/discharging; =0, otherwise).

Equation (42) shows the change of electricity stored in BESS at $t > 1$ in distributed energy storage optimization.

$$\begin{aligned} \widetilde{SOC}^{B}_{MG_{i,t}} = \widetilde{SOC}^{MB}_{MG_{i,t-1}} &+ \frac{1}{E^{B}_{MG_i}}\{(P^{B+}_{MG_{i,t}} + \widetilde{P}^{B+}_{MG_{i,t}}) \cdot \Delta t \cdot \eta^{B+}_{MG_i} \\ &- \frac{(P^{B-}_{MG_{i,t}} + \widetilde{P}^{B-}_{MG_{i,t}}) \cdot \Delta t}{\eta^{B-}_{MG_i}})\} \end{aligned} \quad (42)$$

where $\widetilde{SOC}^{B}_{MG_{i,t}}$ is BESS SOC at time t in distributed energy storage optimization. Here, the initial of SOC in a BESS is constrained by Equation (43).

$$\widetilde{SOC}^{MB}_{MG_{i,t=1}} = SOC^{B}_{MG_{i,t=1}} \quad (43)$$

Equation (44) shows that power surplus, BESS discharging, power shortage (such as bought from the power grid) and CBESS discharging should be balanced with power shortage, BESS charging, power surplus (such as sold to the power grid) and CBESS charging.

$$\sum_{i}^{N}(P^{sur}_{MG_{i,t}} + \widetilde{P}^{B-}_{MG_{i,t}} + \widetilde{P}^{va}_{MG_{i,t}}) \cdot \Delta t + P^{CB-}_t \cdot \Delta t$$

$$= \sum_{i}^{N}(P^{va}_{MG_{i,t}} + \widetilde{P}^{B+}_{MG_{i,t}} + \widetilde{P}^{sur}_{MG_{i,t}}) \cdot \Delta t + P^{CB+}_t \cdot \Delta t \quad (44)$$

2) DISTRIBUTED GENERATION OPTIMIZATION

In this stage, the dispatchable units can produce electrical energy based on the update of shortage power obtained from the first stage. The corresponding power output of CDGs can be queried by entering P^{va}_t into the DGPS.

$$P^{va}_t = \begin{cases} \sum_{i}^{N}\widetilde{P}^{va}_{MG_{i,t}} \\ when \sum_{i}^{N}\widetilde{P}^{va}_{MG_{i,t}} \le (\sum_{i}^{N}P^{CDG\_max}_{MG_{i,t}} + P^{cCDG\_max}_t) \\ \sum_{i}^{N}P^{CDG\_max}_{MG_{i,t}} + P^{cCDG\_max}_t \\ when \sum_{i}^{N}\widetilde{P}^{va}_{MG_{i,t}} > (\sum_{i}^{N}P^{CDG\_max}_{MG_{i,t}} + P^{cCDG\_max}_t) \end{cases} \quad (45)$$

After completing MMG optimization by each MMGA at step 2, MMGA calculates $P^{buy}_{MG_{i,t}}$ and $P^{sell}_{MG_{i,t}}$ according to Algorithm 3.

IV. NUMERICAL SIMULATIONS

In this paper, All MILP-based models developed for simulations of the proposed operation of MMG system have been simulated in MATLAB software with integration of Yalmip and IBM ILOG CPLEX.

A. CASE CONFIGURATION

In order to investigate the proposed strategy for MMG system, we consider the system depicted in Fig. 1 and Table 2 summarizes the major components in the system. BESS parameters in MG and CMG are shown in Table 3. The parameters related to CDGs of each MG and CMG are tabulated in Table 4. The emission coefficient of oil is set as 3.51 tCO_2/m^3 based on the information provided in [27], and the macroeconomic cost of CO_2 reduction is \$598.97/t [28]. The price of diesel oil is set as \$820/m^3 [29].

The forecast output data of PV and WT from the responsibility area of 50Hertz in Germany is used. those data were generated by the weather models(e.g. GFS,ECMWF) and the master data(geographic coordinates, address) of PV and WT [30]. The forecast output power of the renewable power generation was shown in Fig. 7 and Fig. 8.

In this paper, day-ahead total load forecast from three areas (Latvia, Bosnia and Slovakia) of entsoe transparency platform are used [31]. The data of load profile was shown in Fig. 9. In DRP, both $\overline{dr}_{MG_i}$ and $\overline{inc}_{MG_i}$ are assumed to be 20%. It means that only 20% of the MGs' load is shifted, also just 20% increment in the MGs' load is permitted in all time intervals [32].

Typically, the electricity price changes as the demand for electricity changes. day-ahead prices forecast from entsoe transparency platform is plotted in Fig. 10 [31]. For our simulations, we supposed a selling price equal to half the purchasing cost.

Algorithm 3 Computation of MMG Optimization Result

Input: $P^{sur}_{MG_i,t}, P^{va}_{MG_i,t}, P^{B+}_{MG_i,t}, P^{B-}_{MG_i,t}$

Output: $P^{buy}_{MG_i,t}, P^{sell}_{MG_i,t}$

Running Distributed energy storage optimization;

return $\widetilde{P}^{B+}_{MG_i,t}, \widetilde{P}^{B-}_{MG_i,t}, P^{CB+}_t, P^{CB-}_t$;

while $t \leq T$ **do**

  if $\sum_i^N P^{sur}_{MG_{i,t}} \leq \sum_i^N P^{va}_{MG_{i,t}}$ **then**

    $\sum_i^N \widetilde{P}^{va}_{MG_{i,t}} = \sum_i^N (P^{va}_{MG_{i,t}} - P^{sur}_{MG_{i,t}} - \widetilde{P}^{B-}_{MG_{i,t}}) - P^{CB-}_t$;

    $\sum_i^N \widetilde{P}^{sur}_{MG_{i,t}} = 0$;

    if $\sum_i^N \widetilde{P}^{va}_{MG_{i,t}} \leq (\sum_i^N \overline{P}^{CDG}_{MG_i} + \overline{P}^{CCDG})$ **then**

      Running Distributed generation optimization;

      return $P^{CDG}_{MG_i,t}$;

      P^{CCDG}_t;

      $P^{sell}_t = 0$;

      $P^{buy}_t = 0$;

    else

      return $P^{CDG}_{MG_i,t} = \overline{P}^{CDG}_{MG_i}$;

      $P^{CCDG}_t = \overline{P}CCDG$;

      $P^{sell}_t = 0$;

      $P^{buy}_t = \sum_i^N \widetilde{P}^{va}_{MG_{i,t}} - (\sum_i^N \overline{P}^{CDG}_{MG_i} + \overline{P}^{CCDG})$;

    end

  else

    $\sum_i^N \widetilde{P}^{va}_{MG_{i,t}} = 0$;

    $\sum_i^N \widetilde{P}^{sur}_{MG_{i,t}} = \sum_i^N (P^{sur}_{MG_{i,t}} - P^{va}_{MG_{i,t}} - \widetilde{P}^{B+}_{MG_{i,t}}) - P^{CB+}_t$;

    return $P^{CDG}_{MG_i,t} = 0$;

    $P^{CCDG}_t = 0$;

    $P^{sell}_t = \sum_i^N \widetilde{P}^{sur}_{MG_{i,t}}$;

    $P^{buy}_t = 0$;

  end

  t++;

end

B. STEP 1: MG OPTIMIZATION

In this paper, the load participates in DRP, considering the purchase cost and sales profit based on the maximum consumption of renewable energy. Results of the optimization of MG are illustrated in Fig. 11. The figure shows three MGs that have different loads and generation capacity of renewable energy. In Fig. 11(a), the load is less than generation capacity of renewable energy at any time in MG1. Considering

TABLE 2. Components of the MMG system.

No	Name	Type	Quantity	Capacity
MG1	WT	160kW	10	1600kW
	PV	300W	2000	600kW
	CDG	180kW	1	180kW
	BESS	2V/1000Ah	100	200kWh
	Load	-	-	2000kW
MG2	WT	190kW	4	760kW
	PV	410W	1000	410kW
	CDG	160kW	1	160kW
	BESS	2V/2000Ah	45	180kWh
	Load	-	-	1000kW
MG3	WT	200kW	11	2200kW
	PV	300W	5000	1500kW
	CDG	200kW	1	200kW
	BESS	4V/1000Ah	55	220kWh
	Load	-	-	3300kW
Community MG	Community CDG	500kW	1	500kW
	Community BESS	4V/1000Ah	105	420kWh

TABLE 3. Parameters of BESSs in MMG system.

Parameters	Battery energy storage systems			
	MG1	MG2	MG3	MGC
Capacity (kWh)	200	180	220	420
Initial SOC (%)	25	22	27	36
Charging efficiencies (%)	97	96	95	95
Discharging efficiencies (%)	95	98	95	98
The upper limits of BESS charging and discharging power (kW)	150	125	160	200

TABLE 4. Parameters of CDGs in MMG system.

Parameters	Controllable distributed generators			
	MG1	MG2	MG3	MGC
a_1	15	20	12	10
a_2	80	85	75	70
a_3	0	0	0	0
Start-up Cost ($)	15	13	15	14
Ramp-up rate	0.4	0.41	0.43	0.44
Upper limits of CDG power output (kW)	200	180	160	500

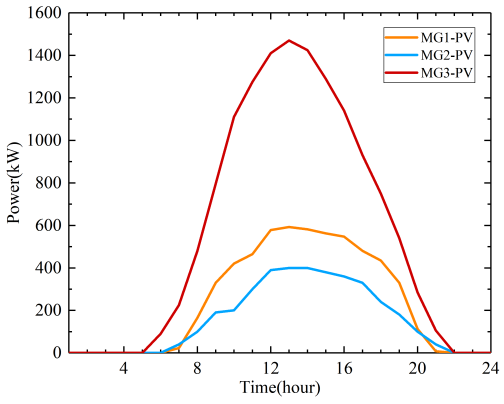

FIGURE 7. The forecast values of PV output power in the 50Hertz grid area.

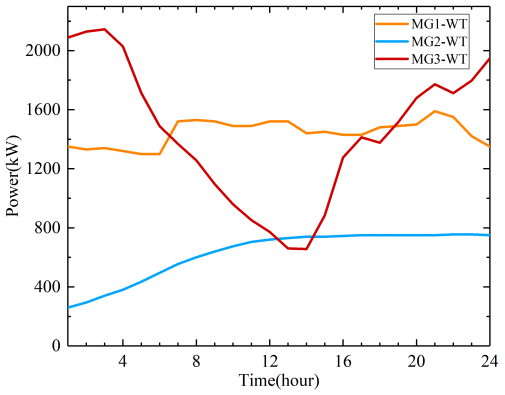

FIGURE 8. The forecast values of WT output power in the 50Hertz grid area.

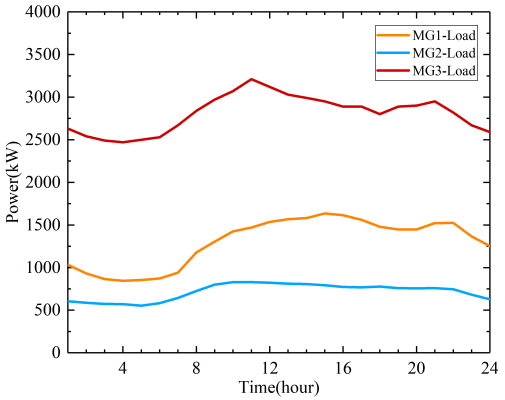

FIGURE 9. The forecast values of hourly load profile.

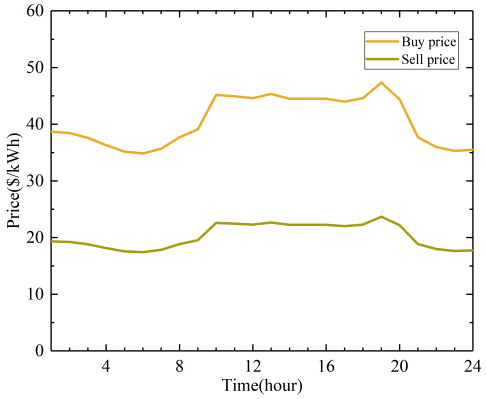

FIGURE 10. The forecast values of hourly grid electricity price.

the surplus sales of renewable energy, the load from the peak price interval is shifted to the off-peak intervals, while ensuring the load demand. Fig. 11(b) shows that the load is shifted as much as possible to the intervals that the generation capacity of renewable energy is more than the load in MG2. The load is more than the generation capacity of renewable energy at any time in MG3, so it needs to buy electricity. According to the electricity price of Fig. 9, load from the peak price interval is shifted to the off-peak intervals after DRP in Fig. 11(c).

TABLE 5. Comparison of result of these cases, (a) MG1, (b) MG2 and (c) MG3.

(a)

MG1	Purchased power (kWh)	Sold power (kWh)	Utilization of renewable energy (%)	Cost(+)/ Profit(-) ($)
Case1-1	0	9049.50	77.54	-185474.72
Case1-2	372.8	9493.67	76.44	-189762.72
Case1-3	0	8966.23	77.75	-193307.35

(b)

MG2	Purchased power (kWh)	Sold power (kWh)	Utilization of renewable energy (%)	Cost(+)/ Profit(-) ($)
Case1-1	1343	2878	84.62	-13034.95
Case1-2	2420.2	4009.7	78.57	2522.13
Case1-3	552.69	1908.76	89.8	-22278.3

(c)

MG3	Purchased power (kWh)	Sold power (kWh)	Utilization of renewable energy (%)	Cost(+)/ Profit(-) ($)
Case1-1	19510	0	100	790458.76
Case1-2	20095.17	666.43	98.6	763416.31
Case1-3	19485.42	0	100	767667.34

The amount of power exchange, utilization of renewable energy, costs, and profits of all MGs are given in Table 5.

It is obvious that the utilization of renewable energy has been improved. Cases 1-3 reduce the amount of purchasing from the power grid or other MGs by making full use of local consumption of renewable energy. At the same time, although the proposed method achieves the lowest power exchange, it still has good results in terms of cost and profit.

In order to elaborate the impact of the proposed strategy, three cases have been compared in MG optimization: (1) case 1-1: optimal scheduling of MG does not consider DRP [33]. (2) case 1-2: optimal scheduling of MG considers DRP, aiming to minimize the operation cost. The operation cost is the difference between purchase price and sales price [19], [21]. (3) case 1-3: The proposed optimal scheduling based on the maximum consumption of renewable energy.

C. STEP 2: MMG OPTIMIZATION

1) DISTRIBUTED ENERGY STORAGE OPTIMIZATION

In order to further consume renewable energy, not only consider CBESS, but also the BESS of each MG are utilized to participate in optimal scheduling of MMG. It can be clearly seen from the Fig. 12 that the power scheduling of MG's BESS in the first step MG optimization and the second step MMG optimization. It is obvious that BESS is fully utilized through 2-steps optimization scheduling.

To verify the effectiveness of the proposed optimal scheduling, four cases are compared: (1) case 2-1: An un coordinated operation strategy. Although the operation of multiple grid-connected MGs are considered, only the interaction between the distribution network and MGs is studied without considering any power exchange among MGs [11], [12], [15], [34]. The system total operation cost is the

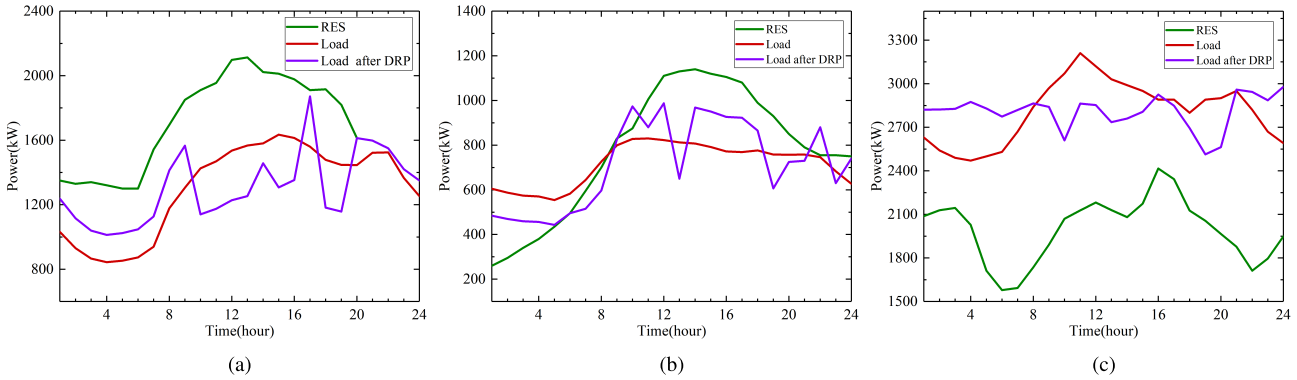

FIGURE 11. Load of MG in response to DRP, (a) MG1, (b) MG2 and (c) MG3.

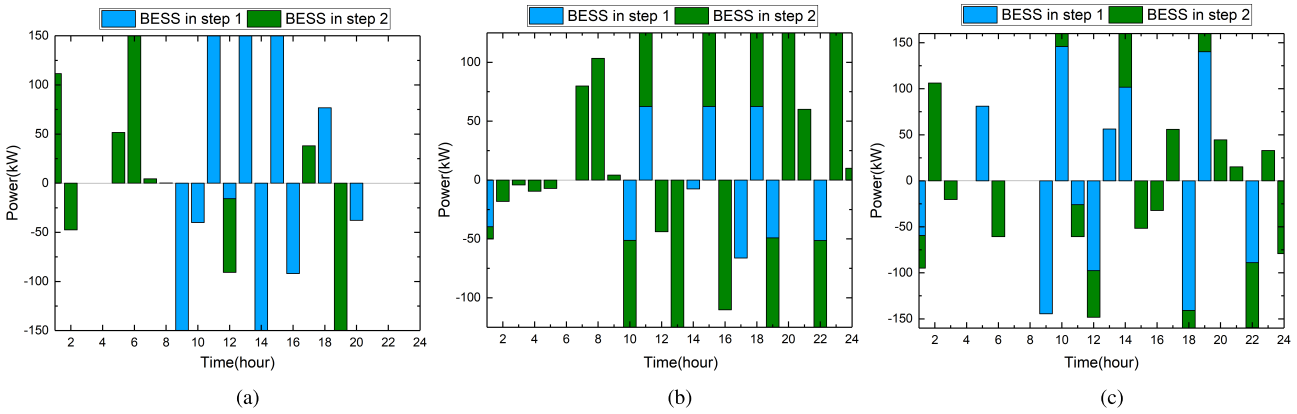

FIGURE 12. Power scheduling of BESS, (a) BESS1, (b) BESS2 and (c) BESS3.

TABLE 6. performance comparison in terms of RES consumption.

MMG	Purchased power (kWh)	Sold power (kWh)	Utilization of renewable energy (%)	Cost(+)/ Profit(-) ($)
Case2-1	20038.10	10874.99	89.8	552081.69
Case2-2	12336.91	3173.80	97.03	387610.95
Case2-3	12228.11	3156.81	97.04	382075.66
Case2-4	10869.66	1991.36	98.14	354072.19

summation of individual's cost. (2) case 2-2: An coordinated operation strategy. In addition to considering the interaction between the distribution network and MGs, power exchange among MGs is also considered [22], [23]. (3) case 2-3: In order to reduce the overall operating cost of MMG system, CBESS is considered [19], [21]. (4) case 2-4: The proposed optimal scheduling based on the maximum consumption of renewable energy.

Fig. 13 demonstrates that buying and selling power between power grid for all the cases. It can be seen from Fig. 13 that the amount of purchased power and sold power has been significantly reduced due to the application of the proposed strategy. Through this strategy, MMG system can make full use of renewable energy and reduce transactions with power grid.

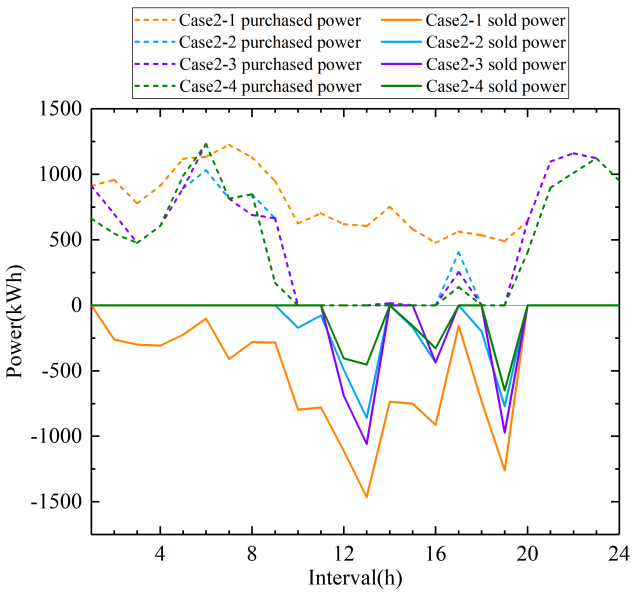

FIGURE 13. Buying and selling amount of electricity in all cases.

The amount of power exchange, utilization of renewable energy, costs, and profits of MMG system are given in Table 6. Obviously, due to share the renewable energy

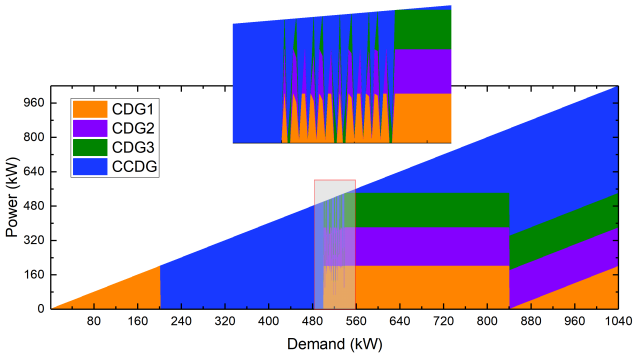

FIGURE 14. The generation schedule of all the CDG in MMG system.

with other MGs, the cost of MMG system is reduced and the utilization of renewable energy is improved.

2) DISTRIBUTED GENERATION OPTIMIZATION

For the shortage of power, first, we get all the CDGs' power generation plans through DGPS, and then power exchang with the power grid.The schedule for the generation of all CDGs in the MMG system is shown in Figure 14.

V. CONCLUSION

In this paper, a new strategy for improving renewable energy local utilization of MMG system through MAS has been proposed. In contrast to the traditional energy management strategy, the BESSs of each MG is also considered by MMG EMS in addition to the CBESS and the CDGs for achieving global optimization. The surplus and shortage power of each MG has been not only compensated by trading power within power grid and the shared distributed energy resources, but also adjusted by exchanging power with other MGs. At the same time, all BESSs participate in the use of renewable energy and the global optimal power generation strategy of all CDGs are enforced, which significantly increases the transactions among MGs. Through these transactions, local utilization of the renewable energy is promoted within the whole MMG system. What's more, in order to maximize renewable energy local consumption, DRP has been taken into consideration and the simulation results proves the improvement effect. In a typical scenario, renewable energy utilization of the entire MMG system is improved by 12.32% using the proposed strategy. Considering big data calculation, this paper proposes optimization strategy based on hierarchical EMS. Simulation results show that, the cooperation of all BESSs is more effective in maximizing renewable energy local consumption and the cooperation of all CDGs is beneficial in reducing the operational cost of MMG system.

REFERENCES

[1] C. Wang, J. Yan, C. Marnay, N. Djilali, E. Dahlquist, J. Wu, and H. Jia, "Distributed energy and microgrids (DEM)," *Appl. Energy*, Vol. 210, pp. 685–689, Jan. 2018. Online]. Available: http://www.sciencedirect.com/science/article/pii/S0306261917316550

[2] F. Farzan, S. Lahiri, M. Kleinberg, K. Gharieh, F. Farzan, and M. Jafari, "Microgrids for fun and profit: The economics of installation investments and operations," *IEEE Power Energy Mag.*, vol. 11, no. 4, pp. 52–58, Jul./Aug. 2013.

[3] Q. Jiang, M. Xue, and G. Geng, "Energy management of microgrid in grid-connected and stand-alone modes," *IEEE Trans. Power Syst.*, vol. 28, no. 3, pp. 3380–3389, Aug. 2013.

[4] T.-C. Ou and C.-M. Hong, "Dynamic operation and control of microgrid hybrid power systems," *Energy*, vol. 66, pp. 314–323, Mar. 2014.

[5] B. Zhang, Q. Li, L. Wang, and W. Feng, "Robust optimization for energy transactions in multi-microgrids under uncertainty," *Appl. Energy*, vol. 217, pp. 346–360, May 2018.

[6] T.-C. Ou, "Ground fault current analysis with a direct building algorithm for microgrid distribution," *Int. J. Electr. Power Energy Syst.*, vol. 53, pp. 867–875, Dec. 2013.

[7] Z. Xu, P. Yang, Y. Zhang, Z. Zeng, C. Zheng, and J. Peng, "Control devices development of multi-microgrids based on hierarchical structure," *IET Gener., Transmiss. Distrib.*, vol. 10, no. 16, pp. 4249–4256, Dec. 2016.

[8] J. Silvente and L. G. Papageorgiou, "An MILP formulation for the optimal management of microgrids with task interruptions," *Appl. Energy*, vol. 206, pp. 1131–1146, Nov. 2017.

[9] X. Jin, J. Wu, Y. Mu, M. Wang, X. Xu, and H. Jia, "Hierarchical microgrid energy management in an office building," *Appl. Energy*, vol. 208, pp. 480–494, Dec. 2017. [Online]. Available: http://www.sciencedirect.com/science/article/pii/S0306261917314150

[10] Z. Wang, B. Chen, J. Wang, M. Begovic, and C. Chen, "Coordinated energy management of networked microgrids in distribution systems," in *Proc. IEEE Power Energy Soc. Gen. Meeting*, Jul. 2015, p. 1.

[11] Z. Wang, B. Chen, J. Wang, and J. Kim, "Decentralized energy management system for networked microgrids in grid-connected and islanded modes," *IEEE Trans. Smart Grid*, vol. 7, no. 2, pp. 1097–1105, Mar. 2016.

[12] T. Lv, Q. Ai, and Y. Zhao, "A bi-level multi-objective optimal operation of grid-connected microgrids," *Electric Power Syst. Res.*, vol. 131, pp. 60–70, Feb. 2016. [Online]. Available: http://www.sciencedirect.com/science/article/pii/S0378779615002898

[13] T. Lv and Q. Ai, "Interactive energy management of networked microgrids-based active distribution system considering large-scale integration of renewable energy resources," *Appl. Energy*, vol. 163, pp. 408–422, Feb. 2016. [Online]. Available: http://www.sciencedirect.com/science/article/pii/S0306261915014294

[14] T. Lu, Z. Wang, Q. Ai, and W.-J. Lee, "Interactive model for energy management of clustered microgrids," *IEEE Trans. Ind. Appl.*, vol. 53, no. 3, pp. 1739–1750, May/Jun. 2017.

[15] W.-J. Ma, J. Wang, V. Gupta, and C. Chen, "Distributed energy management for networked microgrids using online ADMM with regret," *IEEE Trans. Smart Grid*, vol. 9, no. 2, pp. 847–856, Mar. 2018.

[16] J. Wu and X. Guan, "Coordinated multi-microgrids optimal control algorithm for smart distribution management system," *IEEE Trans. Smart Grid*, vol. 4, no. 4, pp. 2174–2181, Dec. 2013.

[17] Y. Han, K. Zhang, H. Li, E. A. A. Coelho, and J. M. Guerrero, "MAS-based distributed coordinated control and optimization in microgrid and microgrid clusters: A comprehensive overview," *IEEE Trans. Power Electron.*, vol. 33, no. 8, pp. 6488–6508, Aug. 2018.

[18] H. S. V. S. K. Nunna and S. Doolla, "Energy management in microgrids using demand response and distributed storage—A multiagent approach," *IEEE Trans. Power Del.*, vol. 28, no. 2, pp. 939–947, Apr. 2013.

[19] V. Bui, A. Hussain, and H.-M. Kim, "A multiagent-based hierarchical energy management strategy for multi-microgrids considering adjustable power and demand response," *IEEE Trans. Smart Grid*, vol. 9, no. 2, pp. 1323–1333, Mar. 2018.

[20] Y. Liu, L. Guo, and C. Wang, "A robust operation-based scheduling optimization for smart distribution networks with multi-microgrids," *Appl. Energy*, vol. 228, pp. 130–140, Oct. 2018. [Online]. Available: http://www.sciencedirect.com/science/article/pii/S0306261918306469

[21] D. Wang, J. Qiu, L. Reedman, K. Meng, and L. L. Lai, "Two-stage energy management for networked microgrids with high renewable penetration," *Appl. Energy*, vol. 226, pp. 39–48, 2018. [Online]. Available: http://www.sciencedirect.com/science/article/pii/S0306261918308328

[22] T. Liu, X. Tan, B. Sun, Y. Wu, and D. H. Tsang, "Energy management of cooperative microgrids: A distributed optimization approach," *Int. J. Elect. Power Energy Syst.*, vol. 96, pp. 335–346, Mar. 2018. [Online]. Available: http://www.sciencedirect.com/science/article/pii/S0142061517300133

[23] L. Che, M. Shahidehpour, A. Alabdulwahab, and Y. Al-Turki, "Hierarchical coordination of a community microgrid with AC and DC microgrids," *IEEE Trans. Smart Grid*, vol. 6, no. 6, pp. 3042–3051, Nov. 2015.
[24] P. Kou, D. Liang, and L. Gao, "Distributed EMPC of multiple microgrids for coordinated stochastic energy management," *Appl. Energy*, vol. 185, pp. 939–952, Jan. 2017. [Online]. Available: http://www.sciencedirect.com/science/article/pii/S0306261916313964
[25] Z. Bao, Q. Zhou, Z. Yang, Q. Yang, L. Xu, and T. Wu, "A multi time-scale and multi energy-type coordinated microgrid scheduling solution—Part I: Model and methodology," *IEEE Trans. Power Syst.*, vol. 30, no. 5, pp. 2257–2266, Sep. 2015.
[26] Y. S. F. Eddy, H. B. Gooi, and S. X. Chen, "Multi-agent system for distributed management of microgrids," *IEEE Trans. Power Syst.*, vol. 30, no. 1, pp. 24–34, Jan. 2015.
[27] L. Tang and P. Che, "Generation scheduling under a CO_2 emission reduction policy in the deregulated market," *IEEE Trans. Eng. Manag.*, vol. 60, no. 2, pp. 386–397, May 2013.
[28] F. H. Aghdam, S. Ghaemi, and N. T. Kalantari, "Evaluation of loss minimization on the energy management of multi-microgrid based smart distribution network in the presence of emission constraints and clean productions," *J. Cleaner Prod.*, vol. 196, pp. 185–201, Sep. 2018. [Online]. Available: http://www.sciencedirect.com/science/article/pii/S0959652618316743
[29] D. Hoad, "Reflections on small island states and the international climate change negotiations (COP21, Paris, 2015)," *Island Stud. J.*, vol. 10, no. 2, pp. 259–262, 2015.
[30] *50Hertz Transmission GmbH [de]*. Accessed: May 3, 2019. [Online]. Available: https://www.50hertz.com/
[31] *Entso Transparency Platform*. Accessed: May 3, 2019. [Online]. Available: https://transparency.entsoe.eu
[32] M. Jalali, K. Zare, and H. Seyedi, "Strategic decision-making of distribution network operator with multi-microgrids considering demand response program," *Energy*, vol. 141, pp. 1059–1071, Dec. 2017.
[33] B. Zhao, X. Zhang, J. Chen, C. Wang, and L. Guo, "Operation optimization of standalone microgrids considering lifetime characteristics of battery energy storage system," *IEEE Trans. Sustain. Energy*, vol. 4, no. 4, pp. 934–943, Oct. 2013.
[34] B. Kim, S. Bae, and H. Kim, "Optimal energy scheduling and transaction mechanism for multiple microgrids," *Energies*, vol. 10, no. 4, p. 566, 2017.

WEI JIANG received the B.S. and M.S. degrees from Xidian University, in 1997 and 2000, respectively, and the Ph.D. degree in communication and information system from Shanghai Jiao Tong University (SJTU), Shanghai, China, in 2008.

She is currently an Associate Professor with the Shanghai University of Electric Power. Her research interests include smart grid, signal processing, and communication.

KAIXU YANG received the B.S. degree in electrical engineering from Changzhou University, Changzhou, China, in 2017. He is currently pursuing the M.S. degree in electrical engineering with the Shanghai University of Electric Power, Shanghai, China.

His research interests include the condition monitoring and the optimization scheduling in microgrid.

JUNJIE YANG received the B.S. and M.S. degrees from the Changchun University of Science and Technology, in 1998 and 2001, respectively, and the Ph.D. degree from Shanghai Jiao Tong University, in 2005.

He is currently a Full Professor with Shanghai Dianji University. His research interests include smart grid, wireless sensor networks, diagnosis of power equipment, and optical networks.

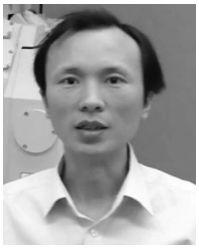

RONGWEI MAO received the B.S. degree from the University of Science and Technology, in 2000, and the Ph.D. degree from the Institute of Semiconductor, Chinese Academy of Sciences, in 2005.

He is currently a Senior Researcher with the University of California Irvine, Irvine. His research interests include smart grid, prototyping, and system integration.

NAIFAN XUE received the B.S. degree in electrical engineering from North China Electric Power University, Beijing, China, in 2016. He is currently pursuing the M.S. degree in electrical engineering with the Shanghai University of Electric Power, Shanghai, China.

His research interests include the condition monitoring and the detection, and location of PD sources in high voltage equipment.

ZHUHANG ZHUO received the B.S. degree in electrical engineering from Wenzhou University, Wenzhou, China, in 2017. He is currently pursuing the M.S. degree in electrical engineering with the Shanghai University of Electric Power, Shanghai, China.

His research interests include the condition monitoring and the optimization scheduling in microgrid.